Title

Reduction of CO2 by Pyridine Monoimine Molybdenum Carbonyl Complexes: Cooperative Metal–Ligand Binding of CO2

Journal

Chemistry - A European Journal, 21(23)

ISSN

0947-6539

Authors

Sieh, Daniel
Lacy, David C
Peters, Jonas C
et al.

Publication Date

2015-06-01

DOI

10.1002/chem.201500463

Peer reviewed

HHS Public Access

Author manuscript

Chemistry. Author manuscript; available in PMC 2016 June 01.

Published in final edited form as:

Chemistry. 2015 June 1; 21(23): 8497–8503. doi:10.1002/chem.201500463.

Reduction of CO_2 by pyridine monoimine molybdenum carbonyl complexes: Cooperative metal-ligand binding of CO_2

Daniel Sieh[a,§], **David C. Lacy**[a,§], **Jonas C. Peters**[a], and **Clifford P. Kubiak**[a,b]

Clifford P. Kubiak: ckubiak@ucsd.edu

[a]Joint Center for Artificial Photosynthesis, Division of Chemistry and Chemical Engineering, California Institute of Technology 1200 East California Boulevard, Pasadena, CA 91125, USA

[b]Department of Chemistry and Biochemistry University of California, San Diego 9500 Gilman Drive MC 0358, La Jolla, California 92093

Abstract

^{Ar}PMI-Mo(CO)$_4$ complexes (PMI = pyridine monoimine; Ar = Ph, 2,6-di-*iso*-propylphenyl) were synthesized and their electrochemical properties were probed with cyclic voltammetry and infrared spectroelectrochemistry (IR-SEC). The complexes exhibit a reduction at more positive potentials than the related bipyridine-Mo(CO)$_4$ complex, which is ligand based according to IR-SEC and DFT data. To probe the reaction product in more detail, stoichiometric chemical reduction and subsequent treatment with CO_2 resulted in the formation of a new product that is assigned as a ligand-bound carboxylate, **[$^{i\mathrm{Pr2Ph}}$PMI-Mo(CO)$_3$(CO$_2$)]$^{2-}$**, by NMR spectroscopic methods. The CO_2 adduct **[$^{i\mathrm{Pr2Ph}}$PMI-Mo(CO)$_3$(CO$_2$)]$^{2-}$** could not be isolated and fully characterized. However, the assignment of the C-C coupling between the CO_2 molecule and the PDI ligand was confirmed by X-ray crystallography of one of the decomposition products of **[$^{i\mathrm{Pr2Ph}}$PMI-Mo(CO)$_3$(CO$_2$)]$^{2-}$**.

Keywords

CO_2 reduction; electrochemistry; spectro-electrochemistry; redox-active ligands; molybdenum

Introduction

Rising levels of atmospheric carbon dioxide threaten global climate change and thus efforts towards renewable solar-energy have stimulated interest in the electrochemical conversion of CO_2 into a solar-fuel. The selective reduction of carbon dioxide to a specific fuel product is currently not possible with heterogeneous electrocatalysts whereas molecular catalysts can, in principle, afford high selectivity. However, the potentials at which CO_2 is reduced with molecular catalysts are usually more negative than −1.8 V vs. Cp_2Fe in acetonitrile and they rarely operate in aqueous media. Therefore, an effort in lowering the overpotential at which CO_2 is reduced represents a challenge in molecular electrocatalysis.[1] Another

Correspondence to: Clifford P. Kubiak, ckubiak@ucsd.edu.

§These authors contributed equally.

Supporting information for this article is given via a link at the end of the document.

advantage of using molecular catalysts is the tunability that is intrinsically available when working with organic/organometallic ligands. Informed choices in new ligands and/or ligand modifications may provide the means to lower the overpotential required to achieve catalysis at high current densities.

A current hypothesis in molecular based CO_2 reduction electrocatalysis is the necessity for so-called ligand redox non-innocence whereby the ligand accepts one or more electrons from a metal centre or an electrode. For example, the bipyridine-$Re(CO)_3$[2,3] system has been thoroughly characterized[4–6] and significant evidence supports the notion that the reduced compound that binds CO_2 is a **[bipy(•)-$Re^0(CO)_3$]$^-$** complex. The redox potential of the metal ion is somewhat fixed within a given ligand framework. However, by tuning the ligand one can change the potentials at which CO_2 is reduced. This has been accomplished previously by modifying the substituents on the bipy ligand.[6,7]

Recently, we and others reported the electrochemical reduction of CO_2 with the related [**bipy-$Mo(CO)_4$**][8] complex and found evidence for electrocatalysis with a formally 18-electron **[bipy-$Mo(CO)_3$]$^{2-}$** complex by reduction of a 19-electron **[bipy(•)-$Mo(CO)_4$]$^-$** at −2.68 V vs. Cp_2Fe.[9,10] This reduction process is likely ligand based and consequently it was rationalized that by switching to an imino-pyridine ligand, a more positive reduction potential would result. This hypothesis is supported by a previous report which directly compared the electronic properties of **[bipy-$Re^I(CO)_3Cl$]** and **[^{Ph}PMA-$Re^I(CO)_3Cl$]** (PMA: pyridine monoaldimine) demonstrating that by exchanging a pyridine moiety for an imine group with an aryl substituent the redox potential of the ligand shifts positive by *ca*. 400 mV.[11] Moreover, there is precedent of pyridine diimine (PDI) supported cobalt based molecular electrocatalysis for CO_2 reduction[12] and it seemed likely that this could be extended to other metal ions. Herein we report our findings using pyridine monoimine $Mo(CO)_4$ precursors (Figure 1) towards electrochemical and stoichiometric CO_2 reduction and show evidence that the fully reduced Mo complex binds the CO_2 carbon atom on the ligand and the oxygen atom on the metal centre.

Results and Discussion

Syntheses and characterization

The phenyl and di-*iso*-propyl derivatives of the pyridine monoimine ligands **^{i}Pr2Ph^{Ph}PMI** and **^{Ph}PMI**, respectively, were synthesized by a condensation reaction with 2-acetylpyridine and the appropriate aniline under azeotropic removal of water in toluene. The complexes **^{i}Pr2Ph^{Ph}PMI-$Mo(CO)_4$** and **^{Ph}PMI-$Mo(CO)_4$** were synthesized by refluxing the appropriate ligand with $Mo(CO)_6$ in toluene. After removal of the solvent, washing the residue with pentane and recrystallization, the complexes **^{i}Pr2Ph^{Ph}PMI-$Mo(CO)_4$** and **^{Ph}PMI-$Mo(CO)_4$** where obtained in 64% and 69% yield, respectively, as analytically pure solids. ^{1}H and ^{13}C NMR spectroscopic characterization of the complexes is consistent with the respective PMI ligand framework and three carbonyl resonances can be detected in the ^{13}C NMR spectra, indicating two equivalent axial and two additional unique carbonyl ligands trans to the PMI ligand and an overall C_s symmetry. In order to compare the electronic properties of the PMI ligands to the parent bipy ligand, the CO stretching frequencies were probed by FTIR spectroscopy (Table 1).

There are no significant differences in the C≡O stretching vibrations of the three complexes, indicating similar electronic properties.

Single crystals suitable for X-ray diffraction experiments could be obtained for **^{Ph}PMI-Mo(CO)$_4$** and **^{iPr2Ph}PMI-Mo(CO)$_4$**. The ORTEP diagram of the molecular structure of **^{iPr2Ph}PMI-Mo(CO)$_4$** is given in Figure 2 with selected bonding parameters in the figure caption. Both complexes exhibit a distorted octahedral geometry, indicated by a bond angle < 180° between the axial carbonyl carbon atoms and the Mo metal centre (C(22)-Mo(1)-C(23): 165–168°). There are no significant differences between the CO bond lengths within the two PMI complexes and **bipy-Mo(CO)$_4$**.[13] The CO ligands trans to N_{py} in the PMI complexes have shorter C-O bond lengths than those in **bipy-Mo(CO)$_4$** (~1.156 Å compared ~1.164 Å) indicating that the PMI ligands are stronger π-acids. However, the difference of ~0.01 Å is too small to make a conclusive statement. For related pyridine diimine ligands, elongation of the imine double bonds and shortening of the exocyclic C-C bonds have been used to quantify the amount of electron transfer to the ligand.[14] Comparing these bond lengths of **^{iPr2Ph}PMI-Mo(CO)$_4$** with the bond distances observed for those of the free ligand,[15] only small changes can be found (N1-C2: **^{iPr2Ph}PMI**: 1.2801(17), **^{iPr2Ph}PMI-Mo(CO)$_4$**: 1.2965(18); C2-C3: **^{iPr2Ph}PMI**: 1.4959(18), **^{iPr2Ph}PMI-Mo(CO)$_4$**: 1.478(2)), indicating that the ligand is essentially neutral in the octahedral Mo tetracarbonyl complexes.

Electrochemistry

The electrochemical properties of the PMI complexes were investigated by cyclic voltammetry (CV) in MeCN (Figure 3). Each complex exhibits a reversible one-electron process assigned to the **^{Ar}PMI-Mo(CO)$_4$** / **[^{Ar}PMI-Mo(CO)$_4$]$^-$** redox couple. We propose that **[^{Ar}PMI-Mo(CO)$_4$]$^-$** is best described as having a ligand anion-radical similar to previously studied bipy[3,5] and PDI[5,16] platforms. This assignment is also favoured in the light of infrared-spectroelectrochemical (IR-SEC) results (vide-infra) and the $E_{1/2}$ values, presented in Table 1, are further evidence for a ligand based reduction in that the process occurs approximately 200 mV more positive than **bipy-Mo(CO)$_4$**. A second irreversible reduction process occurs at −2.35 V for **^{Ph}PMI-Mo(CO)$_4$** and −2.55 V for **^{iPr2Ph}PMI-Mo(CO)$_4$** and this is assigned to forming the fully reduced species **[^{Ar}PMI-Mo(CO)$_3$]$^{2-}$**. The loss of a CO ligand would be consistent with the irreversibility of the CV wave of the second reduction and is further supported by IR and ^{13}C NMR spectroscopy (vide infra) for the chemically reduced complex **^{iPr2Ph}PMI-Mo(CO)$_4$**. Since the shape of the first redox couple does not significantly change in MeCN, even after passing the potential for the second reduction (Figure S16), we cannot make a definite statement about the loss of the CO ligand on the CV time scale.

In CO_2 saturated MeCN solution under an atmosphere of CO_2, a current enhancement is observed for **^{iPr2Ph}PMI-Mo(CO)$_4$** to take place with an onset at approximately −2.4 V and peaks at −2.9 V indicative of catalytic behaviour. However, repeating the scan diminished the current enhancement, which could not be recovered by stirring the solution or introducing more CO_2. Electrochemistry in CO_2 saturated THF did not exhibit significant catalytic current enhancement within the limits of the solvent window for CO_2 saturated

THF (Figure S21). A one hour bulk electrolysis measurement in MeCN at −2.5 V vs. the $Ag/AgNO_3$ reference electrode resulted in formation of CO, but only in 10% Faradaic efficiency (we note that only trace H_2 was formed during this process). The CO observed from the bulk electrolysis is likely due to the formation of **$[^{Ar}$PMI-Mo(CO)$_3]^{2-}$**.

To understand the nature of these electron transfers, we investigated the complex **^{iPr2Ph}PMI-Mo(CO)$_4$** with infrared-spectroelectrochemical methods[17] and the results are shown in Figure 4.

At open circuit potential the IR spectrum of the neutral complex is reproduced in the IR-SEC cell. Upon stepping the potential into the first reduction all four carbonyl stretching vibrations are shifted towards lower frequencies and can now be observed at 1985, 1860, 1843 and 1798 cm^{-1}, indicating stronger back bonding to the carbonyls. The small shift of about 30–40 cm^{-1} however indicates that the reduction is mostly localized at the PMI ligand. At potentials of the second reduction a more drastic change can be observed. Three carbonyl stretching vibrations can now be detected at 1840, 1712 and 1701 cm^{-1}, indicating significantly stronger back bonding. The results of the IR-SEC experiment are in good agreement with the IR data observed for neutral, mono- and doubly-reduced tungsten carbonyl bipyridine complexes obtained by chemical reduction.[9]

Chemical reduction and reaction with CO_2

To gain insight into the electrochemical behaviour of the PMI-Mo complexes in presence of CO_2 we investigated the chemical reduction and subsequent reaction with CO_2. Reduction of the complex **^{iPr2Ph}PMI-Mo(CO)$_4$** was achieved using an excess of KC_8 in [D_8]THF, which led to a quick colour change from red to orange[18] to violet. Attempts to crystallize the rather sensitive orange and/or violet species have been unsuccessful. However, the ^1H and ^{13}C NMR spectra of the violet species suggest the clean formation of a single product that is formulated as **$[^{iPr2Ph}$PMI-Mo(CO)$_3]^{2-}$**. ^1H NMR spectroscopic investigation of the violet product after filtration from graphite revealed a remarkable upfield shift of the resonances of the pyridine protons, which is also evident in some of the ^{13}C NMR resonances. The largest shift can be observed in the imine carbon resonance, which is detected at 172 ppm in the neutral compound and is shifted to 118 ppm in the doubly reduced form. A correlation of upfield shifts of ^{13}C NMR resonances upon electron transfer to the ligand backbone has been previously discussed for PDI complexes.[19] Only one carbonyl resonance can be observed in the ^{13}C NMR spectrum at 245 ppm, which is consistent with the loss of one carbonyl ligand and fast exchange of the remaining three ligands on the NMR time scale at room temperature.[20] Furthermore, the carbonyl resonance is shifted to higher frequencies compared to the neutral parent complex consistent with stronger back bonding to the carbonyl ligands.[21] The loss of one CO ligand is also supported by head space analysis (GC) in one of the reactions, which showed the formation of CO in the order of magnitude of the reaction size. FTIR spectra of freshly prepared solutions of **$[^{iPr2Ph}$PMI-Mo(CO)$_3]^{2-}$** in THF or [D_8]THF provided carbonyl stretching vibrations at 1845, 1719 and 1700 cm^{-1}. These frequencies are nearly identical to the ones observed in the IR-SEC for the doubly reduced species. To further corroborate these stretching frequencies with the IR-SEC data, the chemical reduction was performed in

[D_3]MeCN. Although the NMR spectrum is not as clean as those obtained in THF-d_8 (as expected for KC_8 reduction in MeCN), similar upfield shifts in the ^{1}H NMR spectrum were observed. Additionally, freshly prepared THF solutions **[$^{i\text{Pr2Ph}}$PMI-Mo(CO)$_3$]$^{2-}$** could be stripped of solvent and dissolved in MeCN from which the main features (1840, 1712 and 1701 cm^{-1}) of the IR spectrum obtained by electrochemical reduction were reproduced (Figure S27).

Reaction of the in-situ prepared violet, doubly reduced complex **[$^{i\text{Pr2Ph}}$PMI-Mo(CO)$_3$]$^{2-}$** with CO_2 led to a colour change to pale yellow/brown and ^{1}H NMR spectroscopic investigation of the reaction products revealed the formation of a major product alongside small amounts of unidentified side products. Using Cp*$_2$Fe as an internal standard a NMR-yield of 80(10)% could be established, indicating that the majority of the dianion **[$^{i\text{Pr2Ph}}$PMI-Mo(CO)$_3$]$^{2-}$** is converted to this major product. The presence of two resonances for the methine protons as well as the protons in the 3 and 5 positions and 4 resonances for the *iso*-propyl methyl groups suggest the loss of the mirror plane, which is present in the neutral and reduced parent complexes. The ^{1}H and ^{13}C NMR resonances show significant broadening, which might be attributed to a fluxional process, i.e. K^+ coordination/decoordination. This view is supported by a significant sharpening of the resonances upon addition of 18-crown-6 or recording the NMR spectra in [D_7]DMF of a sample that was originally prepared in THF. A ^{13}C NMR resonance for the CO ligands can be estimated at 236 ppm as a very broad signal (in [D_8]THF and [D_7]DMF) suggesting that the exchange of the three CO ligands is slow compared to the parent compound. Two ^{13}C NMR resonances are observed at 185 and 173 ppm in the region expected for imine-carbon and pyridine-carbon atoms typical for PDI-metal complexes (Figure 5), both of which show coupling to the protons of the methyl group of the parent imine moiety (δ = 1.14 ppm, N-CCH_3) in the ^{1}H,^{13}C HMBC NMR spectrum. The resonance at 185 ppm is strongly enhanced using $^{13}CO_2$ (Figure 5, inset A), suggesting incorporation of the CO_2 carbon atom. Moreover, it indicates that the resonance at 185 ppm is not a PMI ligand resonance. Interestingly, the ^{1}H,^{13}C HMBC NMR spectrum revealed that the methyl protons are also coupled to a ^{13}C NMR resonance at 75 ppm, which is an uncommon shift for a PMI ligand.

This ^{13}C NMR resonance is split into a doublet with a coupling constant of 55 Hz in the ^{13}C labelled compound (figure 5, inset B), which is consistent with coupling to the carbon atom in $^{13}CO_2$ and is in the range of $^1J_{C,C}$ coupling constants for substituted carbonic acid/ester (RO(O=)CR').[22] Furthermore the ^{1}H NMR resonance at δ = 1.14 ppm is split into a doublet with a coupling constant of 3 Hz in the labelled complex (Figure S29), which is not uncommon for a 3 bond C,H coupling.[22]

Taken together, the findings from the NMR spectroscopic investigation of the product obtained by treating **[$^{i\text{Pr2Ph}}$PMI-Mo(CO)$_3$]$^{2-}$** with CO_2 is consistent with the formation of a CO_2 adduct in which the CO_2 carbon atom binds to the imine carbon atom of the reduced complex and is thus formulated as **[$^{i\text{Pr2Ph}}$PMI-Mo(CO)$_3$(CO$_2$)]$^{2-}$** (Scheme 1).

Albeit unusual, this type of ligand-centered CO_2 binding mode has been observed before. For example, Braunstein *et al.* in 1981 obtained a similar result to ours by activation of CO_2 at a square planar Pd diphenylphophinoacetate complex.[23] Similar binding patterns of

carbon dioxide have recently been reported for PNN-Ru[24] and PNP-Ru/Re[25] pincer complexes as well as β-diketiminate Sc[26] complexes.

Keeping the CO_2 adduct in [D_8]THF under an atmosphere of CO_2 causes decomposition with a half-life of about one day. Multiple, so far unidentified products were observed following this process by ^{1}H NMR spectroscopy. Removal of the solvent and the CO_2 atmosphere, followed by dissolution in fresh [D_8]THF enhanced the stability of the CO_2 adduct. This sample showed significantly less decomposition as monitored by ^{1}H NMR spectroscopy over the course of several days. However, attempts to crystallize or isolate **[*i*^{Pr2Ph}PMI-Mo(CO)$_3$(CO$_2$)]$^{2-}$** led to decomposition. Crystals that grew from a THF solution at −35°C provided strong evidence for the C-C bond formation between the former imine carbon atom and the CO_2 carbon atom (Figure 6). Only one potassium atom could be located in the Fourier density maps, indicating that the (diamagnetic) CO_2 adduct **[*i*^{Pr2Ph}PMI-Mo(CO)$_3$(CO$_2$)]$^{2-}$** observed by NMR spectroscopy either underwent an oxidative process to form a **[*i*^{Pr2Ph}PMI-Mo(CO)$_3$(CO$_2$)]$^-$** 19 e$^-$ radical monoanion or, more likely, that the charge is compensated by a proton instead of a potassium cation. The most likely protonation site would be the former imine nitrogen atom. Accordingly, refining a hydrogen atom on the former imine nitrogen atom N1 resulted in a stable refinement with almost equal Rvalues and bonding parameters than without the H atom. Since the presence of a hydrogen atom is not provable by X-ray diffraction alone, the data without the hydrogen atom are presented below and briefly discussed, since the structural data provide additional proof for the C-C coupling that was proposed based on the NMR data.[27] A comparison of both solutions is provided in the supporting information. The central molybdenum ion exhibits a strongly distorted octahedral coordination geometry. Noteworthy is the long molybdenum nitrogen bond length Mo(1)-N(1) of 2.365(3) Å. The molybdenum metal is also bound to one of the former CO_2 oxygen atoms O(4). The bond length Mo(1)-O(4) of 2.238(2) Å is also rather long and consistent with the slow exchange of the three remaining CO ligands observed by ^{13}C NMR spectroscopy. The carbon atom (C(23)) of the former CO_2 molecule is bound to the former imine carbon atom (C(2)) of the PMI ligand and the bond length of 1.572(5) Å is in the order of a C-C single bond.

The CO_2 molecule is bent and with a sum of angles of 360° the carbon atom C(23) is sp^2 hybridized. Consequentially, the C-O bond lengths C(23)-O(4) (1.273(4) Å) and C(23)-O(5) (1.230(4) Å) are consistent with a delocalized C-O double bond and a small preference for the oxygen atom that is not bound to the molybdenum metal centre.[28] With angles between 102 and 114°, the former imine carbon atom C(2) is sp^3 hybridized and the N(1)-C(2) (1.527(5) Å) and the C(2)-C(3) (1.523(5) Å) bond distances indicate single bonds.[28,29] The potassium ion is coordinated by the carboxylate oxygen atom O(4) and O(5), as well as two THF molecules. The coordination sphere is saturated by two oxygen atoms (O(2) and O(5)) of neighbouring molecules (see Figure S41).

Despite the incomplete CO_2 reduction in the bulk electrolysis experiment, we investigated the possibility that the carbon atom in the CO_2 adduct could scramble into the carbonyl ligands on the molybdenum ion. However, the ^{13}C NMR resonance of free CO is observed at 185 ppm in [D_8]THF[30] and thus overlaps with the resonance of that in **[*i*^{Pr2Ph}PMI-Mo(CO)$_3$(CO$_2$)]$^{2-}$**. Nonetheless, no signal enhancement was observed in the resonance at

236 ppm, which is assigned to the carbonyl ligands of **[*i*Pr2PhPMI-Mo(CO)$_3$(CO$_2$)]$^{2-}$** (Figure 5, inset A). The aforementioned formation of side and/or decomposition products indicated by inspection of the ^{1}H NMR spectrum is confirmed by the ^{13}C NMR spectrum of the reaction product(s) in the $^{13}CO_2$ experiment, where ^{13}C incorporation into several products can be observed.

DFT calculations of the reduced complexes

The complex **[*i*Pr2PhPMI-Mo(CO)$_3$(CO$_2$)]$^{2-}$** is not indefinitely stable and attempts to isolate the complex were unsuccessful due to decomposition. Neither were we successful at reliably generating the species in an IR cell in order to corroborate IR data. In order to gain additional insights into the structure of the CO_2 reduction product, we performed a series of DFT calculations starting with the crystal coordinates of the ***i*Pr2PhPMI-Mo(CO)$_4$** precursor. The bond distances obtained by DFT are in reasonable agreement with those obtained from the molecular structure and are tabulated in Table S11. The lowest unoccupied molecular orbital (LUMO) of ***i*Pr2PhPMI-Mo(CO)$_4$** is primarily located on the ligand backbone (Figure S43). Not surprisingly, inspection of the highest singly occupied molecular orbital (SOMO) and the Mulliken spin-density surface of the one-electron reduced species "**[*i*Pr2PhPMI-Mo(CO)$_4$]$^-$**" reveals that the reducing equivalent is predominantly on the ligand and overlays almost identically to the LUMO of **[*i*Pr2PhPMI-Mo(CO)$_4$]** (Figure S44). Earlier we hypothesized, in agreement with the ^{13}C NMR and FTIR data, that the second reduction of ***i*Pr2PhPMI-Mo(CO)$_4$** results in loss of a CO ligand and thus optimized the twice reduced species as **[*i*Pr2PhPMI-Mo(CO)$_3$]$^{2-}$** (Figure 7 and S45).

Again, inspection of the frontier orbitals reveals predominantly ligand-based reductions. These ligand-based reductions are also evident by a lengthening of the imine C-N bond lengths from 1.332 Å in the optimized structure of **[*i*Pr2PhPMI-Mo(CO)$_4$]** to 1.370 Å in **[*i*Pr2PhPMI-Mo(CO)$_4$]$^-$** and 1.421 Å in **[*i*Pr2PhPMI-Mo(CO)$_3$]$^{2-}$**. These changes in bond lengths are accompanied by contraction of the C-C bond that links the imine carbon to the pyridine moiety corresponding to more double bond character (1.453 Å to 1.419 Å to 1.392 Å). These changes in bond lengths upon ligand reduction are well established in the PDI literature. It is less established for pyridine monoketimine complexes but has been discussed for some pyridine monoaldimine complexes.[31] We also optimized the CO_2 adduct species with the carbon atom from CO_2 bonded directly to the carbon atom of the imine group (C_{im}) (Figure S46). The frontier orbitals of this optimized structure resemble the neutral tetracarbonyl precursor as opposed to the dianion complex. We take this as support for the hypothesis that the reducing equivalents that ultimately attack CO_2 reside on the ligand, rather than the Mo centre. We performed frequency calculations on all four of these geometry optimized structures to obtain vibrational spectra and compared them to those we obtained in the IR/IR-SEC experiments. The overall patterns for the CO stretching vibrations derived by DFT methods for the tetracarbonyl starting material, as well as the mono- and doubly reduced complexes are in good agreement with the experimentally observed ones (Figure S47–S49). As mentioned earlier, we were unable to reliably prepare IR samples of the CO_2 adduct **[*i*Pr2PhPMI-Mo(CO)$_3$(CO$_2$)]$^{2-}$**. However, FTIR spectra in

MeCN and THF show close similarities with the one derived by DFT methods for the proposed structure, as presented in the supporting material (Figure S50 and S51).

Conclusions

In summary we have synthesised and fully characterized the two pyridine monoamine (PMI) molybdenum tetracarbonyl complexes **[^{Ph}PMI-Mo(CO)$_4$]** and **[^{iPr2Ph}PMI-Mo(CO)$_4$]**. These complexes were investigated for electrocatalytic CO_2 reduction and compared to the parent **bipy-M(CO)$_4$** system (M = Cr, Mo, W). In order to gain further insight into the reduction product with CO_2, we used stoichiometric reductant to produce **[^{iPr2Ph}PMI-Mo(CO)$_3$]$^{2-}$**. Subsequent treatment with CO_2 resulted in the formation of a new adduct that displays cooperative interaction of the metal centre and the ligand with CO_2. The NMR spectroscopic investigation provides strong evidence for the proposed structure of **[^{iPr2Ph}PMI-Mo(CO)$_3$(CO$_2$)]$^{2-}$** in which the CO_2 carbon atom binds to the imine carbon atom. This structural assignment is further corroborated DFT calculations. In contrast to other PDI cobalt or iron based systems, which appear to be highly covalent, the molybdenum complexes studied here have a fully separated ligand-based reduction. This manifests in the extremely negative potentials required to access the fully reduced states that react with CO_2. Additionally, the formation of a strong C–C bond between CO_2 and PMI ligand is likely deleterious to catalytic turnover. We are currently investigating the use of the PMI ligands with rhenium and manganese in hopes of driving electrocatalytic CO_2 reduction at more positive potentials.

Supplementary Material

Refer to Web version on PubMed Central for supplementary material.

Acknowledgements

This material is based upon work performed by the Joint Center for Artificial Photosynthesis, a DOE Energy Innovation Hub, supported through the Office of Science of the U.S. Department of Energy under Award Number DE-SC0004993. David C. Lacy is supported by the National Institutes of Health (Award Number F32GM106726). The authors thank Michael Takase and Lawrence M. Henling for help with the absorption correction of the X-ray data and David VanderVelde for helpful discussions concerning NMR spectroscopy. Jesse D. Froehlich, Charles W. Machan and Matthew D. Sampson are thanked for the introduction to IR-SEC techniques.

References

1. a) Benson EE, Kubiak CP, Sathrum AJ, Smieja JM. Chem. Soc. Rev. 2009; 38:89–99. [PubMed: 19088968] b) Kumar B, Llorente M, Froehlich J, Dang T, Sathrum A, Kubiak CP. Annu. Rev. Phys. Chem. 2012; 63:541–569. [PubMed: 22404587] c) Finn C, Schnittger S, Yellowlees LJ, Love JB. Chem. Commun. 2012; 48:1392–1399.d) Windle CD, Perutz RN. Coord. Chem. Rev. 2012; 256:2562–2570.e) Costentin C, Robert M, Saveant J-M. Chem. Soc. Rev. 2013; 42:2423–2436. [PubMed: 23232552] f) Appel AM, Bercaw JE, Bocarsly AB, Dobbek H, DuBois DL, Dupuis M, Ferry JG, Fujita E, Hille R, Kenis PJA, Kerfeld CA, Morris RH, Peden CHF, Portis AR, Ragsdale SW, Rauchfuss TB, Reek JNH, Seefeldt LC, Thauer RK, Waldrop GL. Chem. Rev. 2013; 113:6621–6658. [PubMed: 23767781]
2. Hawecker J, Lehn J-M, Ziessel R. J. Chem. Soc., Chem. Commun. 1984:328–330.
3. Sullivan BP, Bolinger CM, Conrad D, Vining WJ, Meyer TJ. J. Chem. Soc., Chem. Commun. 1985:1414–1416.

4. a) Christensen P, Hamnett A, Muir AVG, Timney JA. J. Chem. Soc., Dalton Trans. 1992:1455–1463.b) Johnson FPA, George MW, Hartl F, Turner JJ. Organometallics. 1996; 15:3374–3387.c) Smieja JM, Benson EE, Kumar B, Grice KA, Seu CS, Miller AJM, Mayer JM, Kubiak CP. Proc. Natl. Acad. of Sci. U. S. A. 2012; 109:15646–15650. [PubMed: 22652573] d) Grice KA, Gu NX, Sampson MD, Kubiak CP. Dalton Trans. 2013; 42:8498–8503. [PubMed: 23629511] e) Benson EE, Sampson MD, Grice KA, Smieja JM, Froehlich JD, Friebel D, Keith JA, Carter EA, Nilsson A, Kubiak CP. Angew. Chem. Int. Ed. 2013; 52:4841–4844.f) Sampson MD, Froehlich JD, Smieja JM, Benson EE, Sharp ID, Kubiak CP. Energy Environ. Sci. 2013; 6:3748–3755.g) Grice, KA.; Kubiak, CP. Advances in Inorganic Chemistry : CO_2 Chemistry. Aresta, M.; Eldik, Rv, editors. Vol. 66. Academic Press; 2014. p. 163-188.
5. Stor GJ, Hartl F, van Outersterp JWM, Stufkens DJ. Organometallics. 1995; 14:1115–1131.
6. Smieja JM, Kubiak CP. Inorg. Chem. 2010; 49:9283–9289. [PubMed: 20845978]
7. Sampson MD, Nguyen AD, Grice KA, Moore CE, Rheingold AL, Kubiak CP. J. Am. Chem. Soc. 2014; 136:5460–5471. [PubMed: 24641545]
8. Stiddard MHB. J. Chem. Soc. 1962:4712–4715.
9. Clark ML, Grice KA, Moore CE, Rheingold AL, Kubiak CP. Chem. Sci. 2014; 5:1894–1900.
10. Tory J, Setterfield-Price B, Dryfe RAW, Hartl F. CHEMELECTROCHEM. 2014
11. Dominey RN, Hauser B, Hubbard J, Dunham J. Inorg. Chem. 1991; 30:4754–4758.
12. Lacy DC, McCrory CCL, Peters JC. Inorg. Chem. 2014; 53:4980–4988. [PubMed: 24773584]
13. Braga SS, Coelho AC, Goncalves IS, Almeida Paz FA. Acta Crystallogr., Sect. E: Struct. Rep. Online. 2007; 63:m780–m782.
14. a) de Bruin B, Bill E, Bothe E, Weyhermüller T, Wieghardt K. Inorg. Chem. 2000; 39:2936–2947. [PubMed: 11232835] b) Budzelaar PHM, de Bruin B, Gal AW, Wieghardt K, van Lenthe JH. Inorg. Chem. 2001; 40:4649–4655. [PubMed: 11511211] c) Knijnenburg Q, Gambarotta S, Budzelaar PHM. Dalton Trans. 2006:5442–5448. [PubMed: 17117213]
15. Nienkemper K, Kotov VV, Kehr G, Erker G, Fröhlich R. Eur. J. Inorg. Chem. 2006:366–379.
16. Lewis J, Schroder M. J. Chem. Soc., Dalton Trans. 1982:1085–1089.
17. a) Best SP, Clark RJH, McQueen RCS, Cooney RP. Review of Scientific Instruments. 1987; 58:2071–2074.b) Ashley K, Pons S. Chem. Rev. 1988; 88:673–695.c) Bullock JP, Mann KR. Inorg. Chem. 1989; 28:4006–4011.d) Machan CW, Sampson MD, Chabolla SA, Dang T, Kubiak CP. Organometallics. 2014; 33:4550–4559.
18. The orange solution also formed when a sodium metal or Na/Hg was used as the reductant. NMR spectroscopic investigation indicated a paramagnetic product, which is therefore assigned to the putative monoanion **[^{i}Pr2Ph$^{}$PMI-Mo(CO)$_4$]$^{-}$**, which was not further investigated in this study.
19. Sieh D, Schlimm M, Andernach L, Angersbach F, Nückel S, Schöffel J, Šušnjar N, Burger P. Eur. J. Inorg. Chem. 2012:444–462.
20. Leibfritz D, tom Dieck H. J. Organomet. Chem. 1976; 105:255–261.
21. a) Todd LJ, Wilkinson JR, Hickey JP, Beach DL, Barnett KW. J. Organomet. Chem. 1978; 154:151–157.b) Lauterbur PC, King RB. J. Am. Chem. Soc. 1965; 87:3266–3267.
22. Kalinoswki, H-O.; Berger, S.; Braun, S. Carbon-13 NMR Spectroscopy. New York: Wiley, Chichester; 1988.
23. Braunstein P, Matt D, Dusausoy Y, Fischer J, Mitschler A, Ricard L. J. Am. Chem. Soc. 1981; 103:5115–5125.
24. Huff CA, Kampf JW, Sanford MS. Organometallics. 2012; 31:4643–4645.
25. a) Vogt M, Gargir M, Iron MA, Diskin-Posner Y, Ben-David Y, Milstein D. Chem. Eur. J. 2012; 18:9194–9197. [PubMed: 22736579] b) Vogt M, Nerush A, Diskin-Posner Y, Ben-David Y, Milstein D. Chem. Sci. 2014; 5:2043–2051.c) Filonenko GA, Conley MP, Copéret C, Lutz M, Hensen EJM, Pidko EA. ACS Catal. 2013; 3:2522–2526.
26. LeBlanc FA, Berkefeld A, Piers WE, Parvez M. Organometallics. 2012; 31:810–818.
27. A protonation of the imine nitrogen atom is, however, supported by resonances at 6.03 and 5.50 ppm, that could be detected in the ^{1}H NMR spectrum crystalline material (see Figure S37).
28. Allen FH, Kennard O, Watson DG, Brammer L, Orpen AG, Taylor R. J. Chem. Soc., Perkin Trans. 2. 1987:S1–S19.

29. Note that the rather long C-N bond length of 1.527(5) Å might also be indicative of a protonated nitrogen atom.

30. a) Sellmann D, Prakash R, Heinemann FW. Eur. J. Inorg. Chem. 2004:1847–1858.b) Blanco C, Godard C, Zangrando E, Ruiz A, Claver C. Dalton Trans. 2012; 41:6980–6991. [PubMed: 22535338]

31. a) Lu CC, Bill E, Weyhermüller T, Bothe E, Wieghardt K. J. Am. Chem. Soc. 2008; 130:3181–3197. [PubMed: 18284242] b) Lu CC, Weyhermüller T, Bill E, Wieghardt K. Inorg. Chem. 2009; 48:6055–6064. [PubMed: 20507103] c) van Gastel M, Lu CC, Wieghardt K, Lubitz W. Inorg. Chem. 2009; 48:2626–2632. [PubMed: 19267507] d) Myers TW, Kazem N, Stoll S, Britt RD, Shanmugam M, Berben LA. J. Am. Chem. Soc. 2011; 133:8662–8672. [PubMed: 21568319] e) Myers TW, Yee GM, Berben LA. Eur. J. Inorg. Chem. 2013:3831–3835.

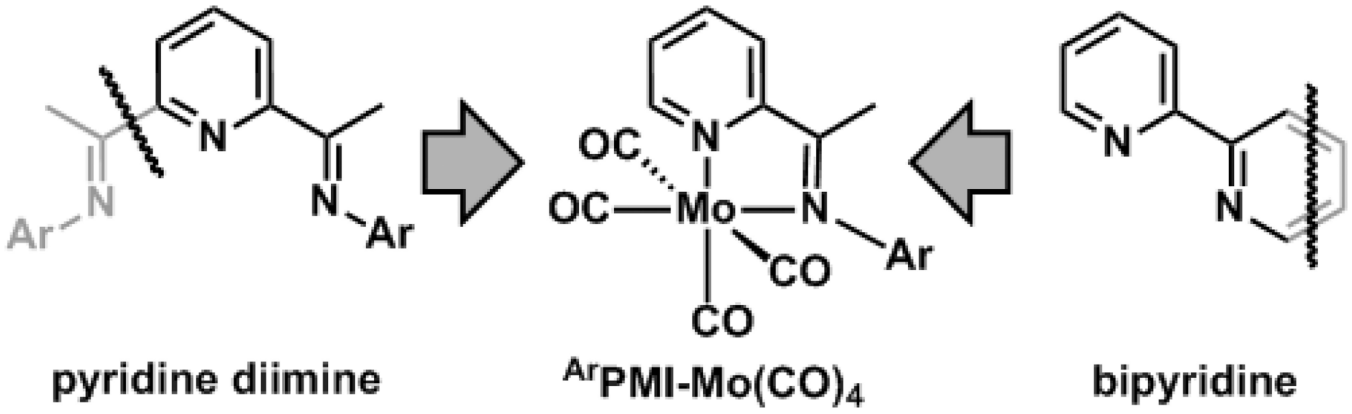

Figure 1.

Inspiration for utilization of the pyridine monoimine ligands (^{Ar}PMI, Ar = Ph, 2,6-di-*iso*-propylphenyl) derived from CO_2 reduction catalysts, which used bipyridine and pyridine diimine moieties.

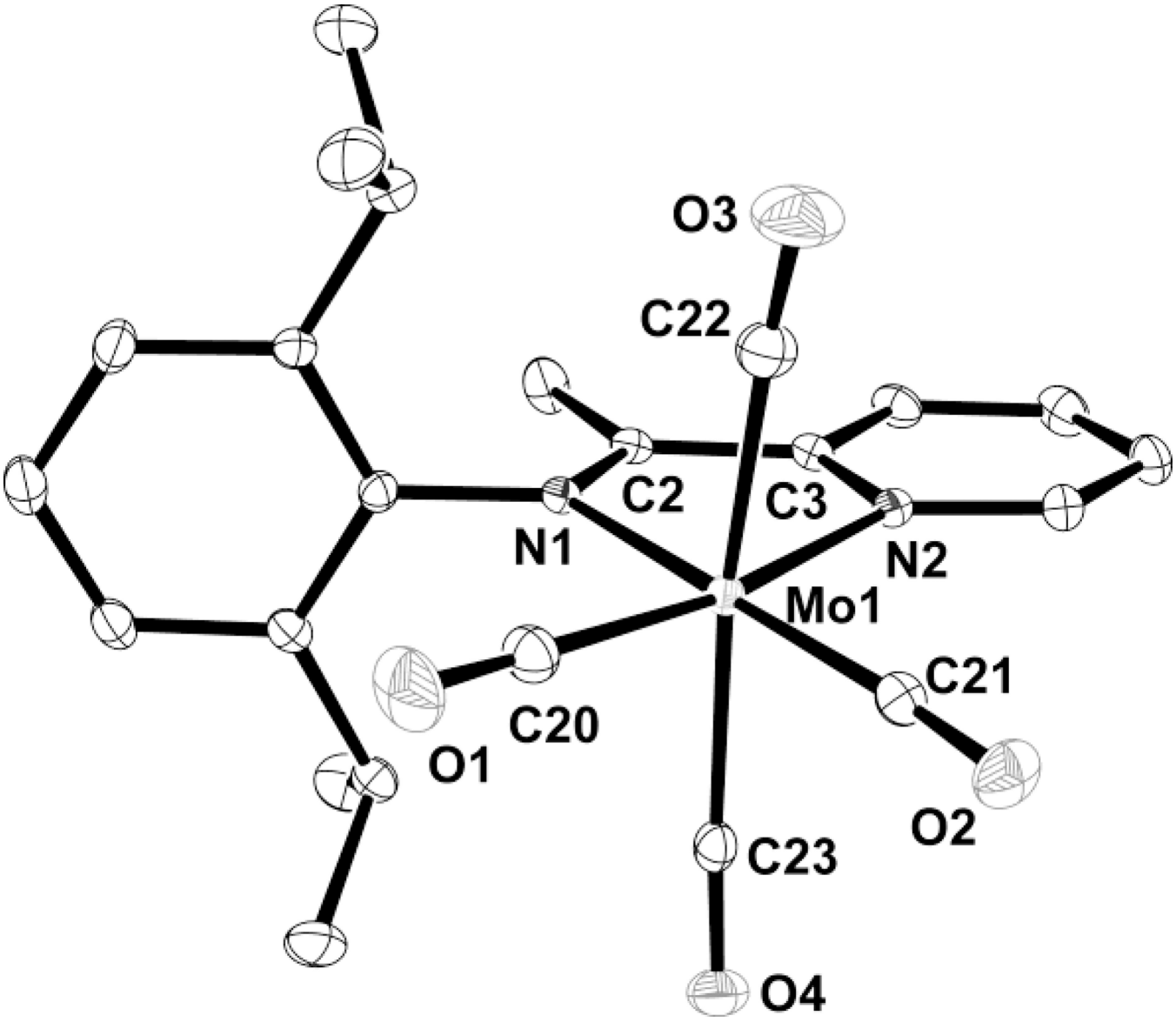

Figure 2.

Ortep diagram of the molecular structure of $^{i\mathrm{Pr2Ph}}$**PMI-Mo(CO)$_4$** with ellipsoids shown at the 50% probability level. Hydrogen atoms are omitted for clarity. Selected bond length (Å) and angles (°) for one of the two independent molecules in the asymmetric unit: Mo(1)-N(1) 2.2453(13), Mo(1)-N(2) 2.2465(12), Mo(1)-C(20) 1.9702(16), Mo(1)-C(21) 1.9568(16), Mo(1)-C(22) 2.0621(19), Mo(1)-C(23) 2.0326(17), C(20)-O(1) 1.1561(19), C(21)-O(2) 1.167(2), C(22)-O(3) 1.140(2), C(23)-O(4) 1.153(2), N(1)-C(2) 1.2965(18), C(2)-C(3) 1.478(2), N(1)-Mo(1)-C(21) 173.89(6), N(2)-Mo(1)-C(20) 169.45(6), N(1)-Mo(1)-N(2) 71.69(5), N(2)-Mo(1)-C(21) 103.11(6), N(1)-Mo(1)-C(20) 98.01(6), C(20)-Mo(1)-C(21) 87.30(7), C(22)-Mo(1)-C(23) 168.41(7), Mo(1)-C(20)-O(1) 179.35(18), Mo(1)-C(21)-O(2) 176.26(15), Mo(1)-C(22)-O(3) 173.64(17), Mo(1)-C(23)-O(4) 171.33(14).

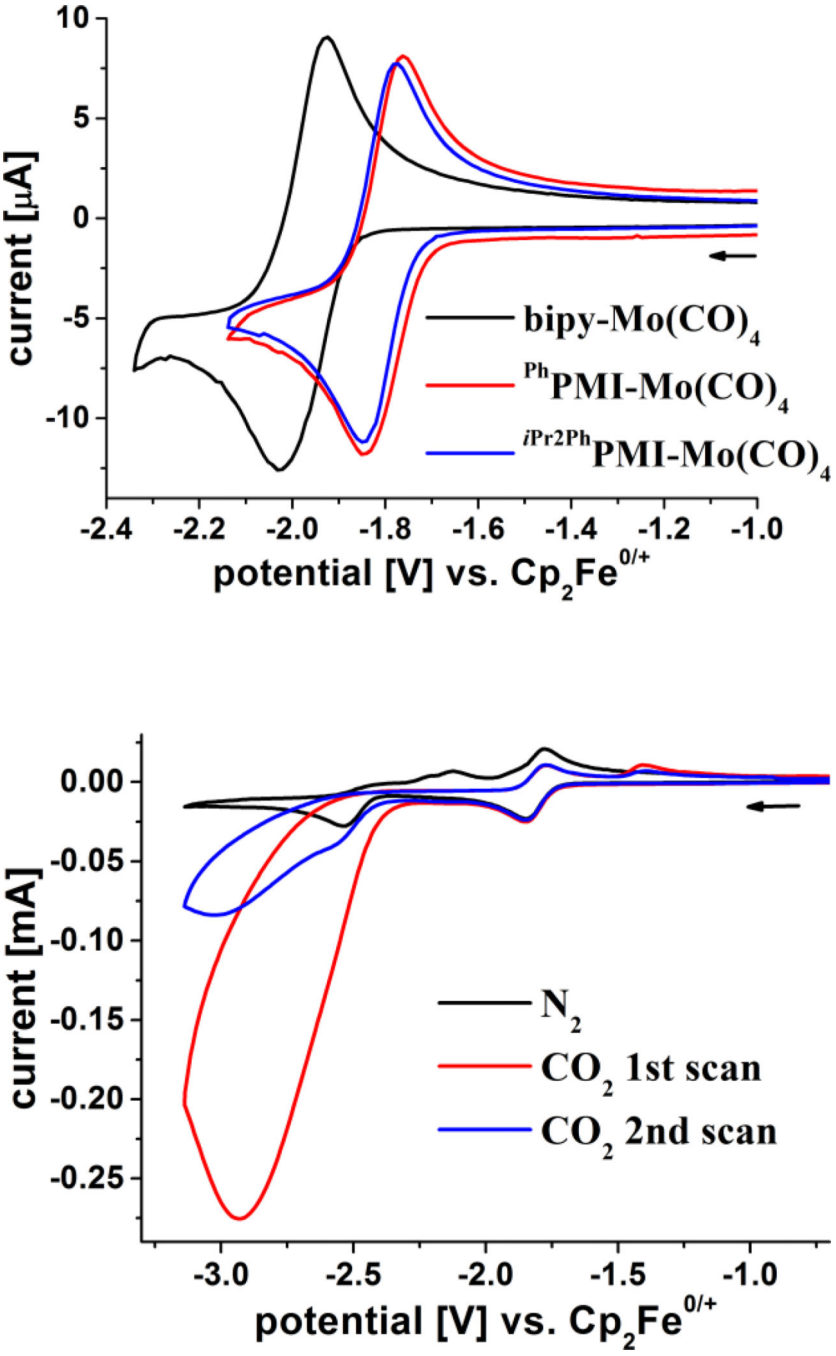

Figure 3.

Cyclic voltammograms of **^{iPr2Ph}PMI-Mo(CO)$_4$** in MeCN in the presence and absence of CO_2 (bottom, 200 mV/s) and a comparison of the isolated reversible reduction for **bipy-Mo(CO)$_4$**, **^{iPr2Ph}PMI-Mo(CO)$_4$**, and **^{Ph}PMI-Mo(CO)$_4$** (top, 100 mV/s). Conditions: 0.1 M [*n*Bu$_4$N]PF$_6$; working electrode = glassy carbon; auxiliary electrode = carbon rod; reference electrode = Ag/AgNO$_3$ (1 mM) in an isolated chamber with 0.1 M [*n*Bu$_4$N]PF$_6$ separated with a Vycor tip.

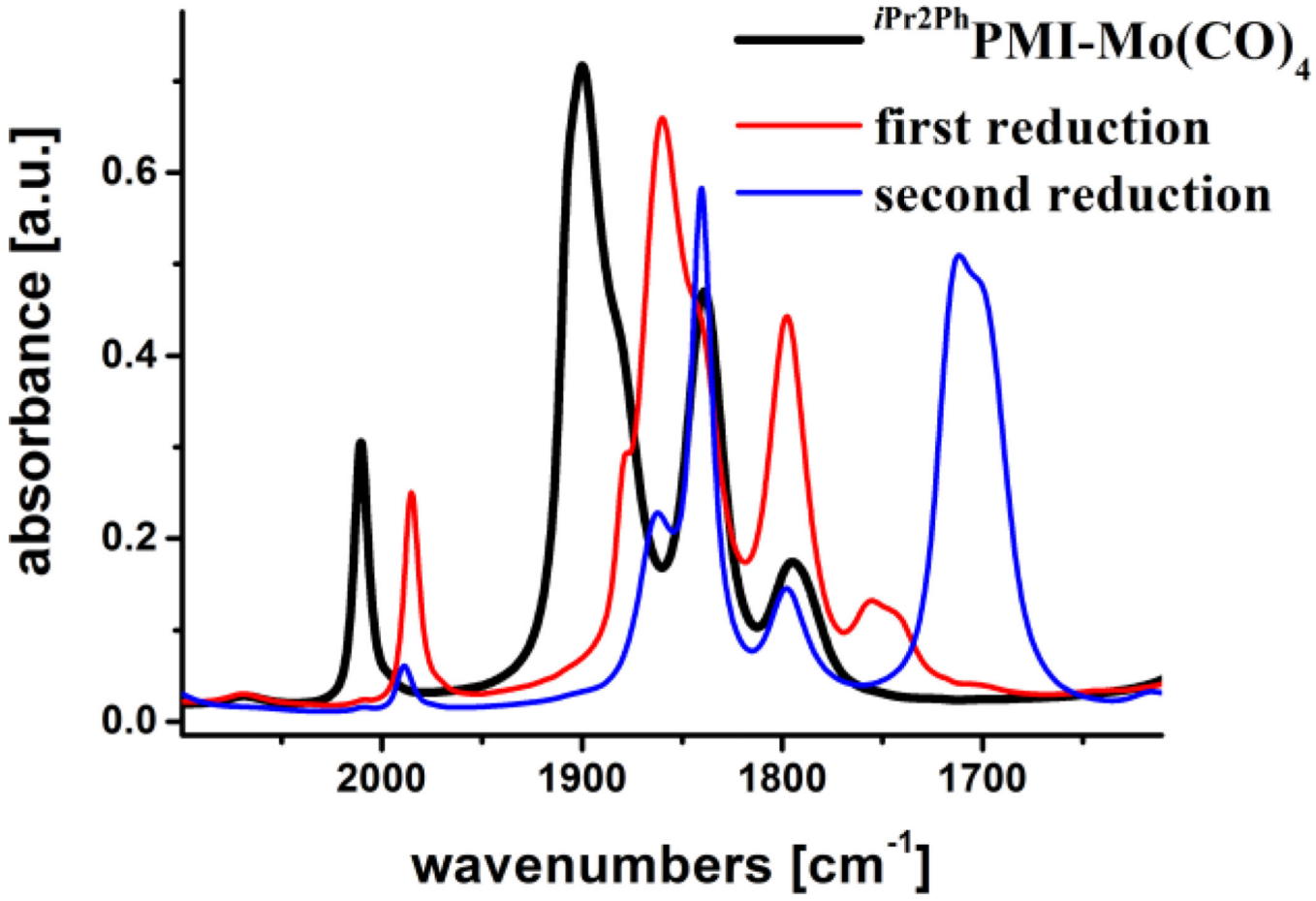

Figure 4.

C≡O region of the IR spectra derived from the IR-SEC experiment. Conditions: 0.1 M [*n*Bu_4N]PF_6 in MeCN; working electrode = Ag; auxiliary electrode = Pt; pseudo reference electrode = Ag.

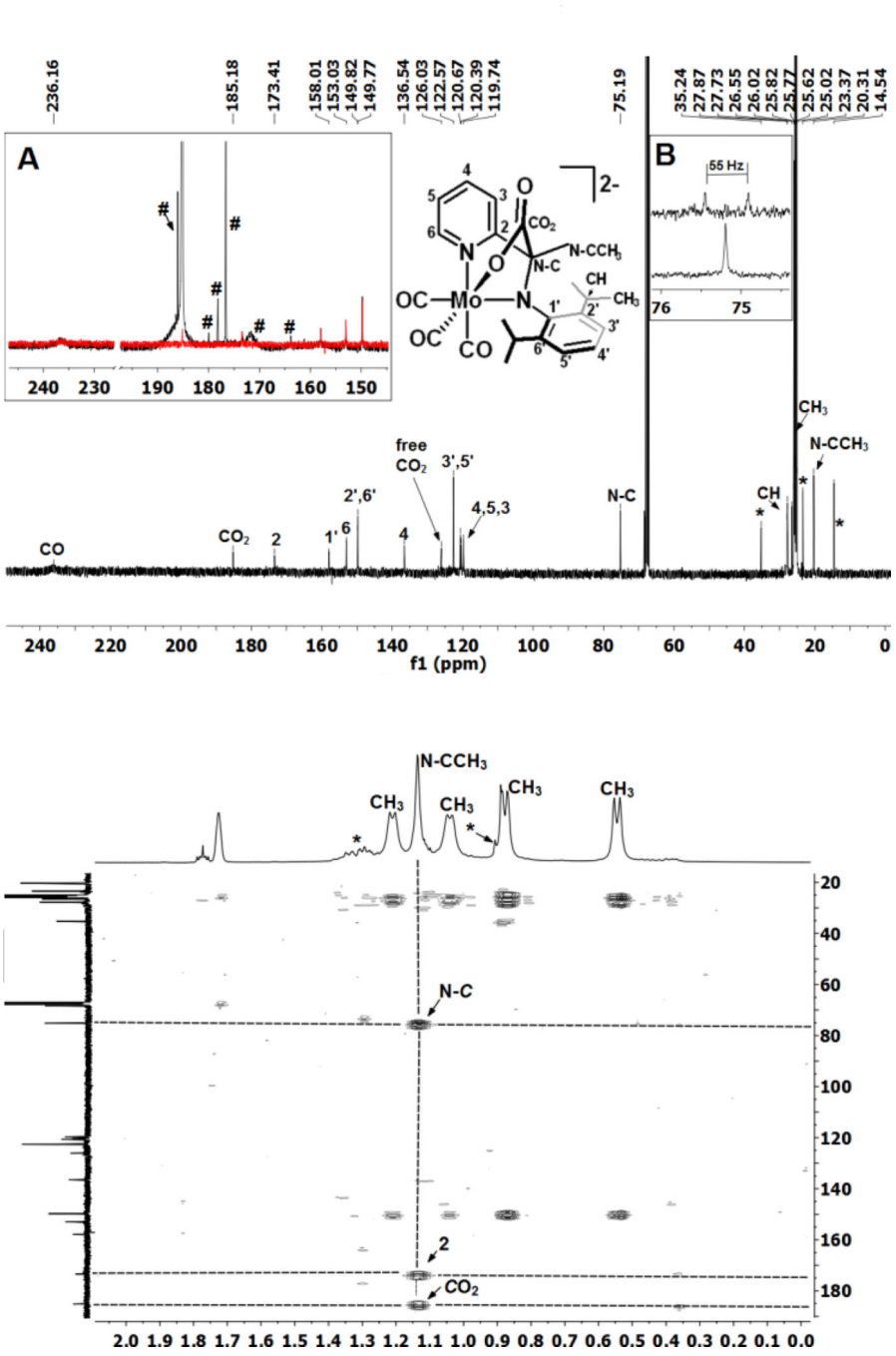

Figure 5.

NMR spectroscopic characterization of the product of the reaction of **[^{i}Pr2PhPMI-Mo(CO)$_4$]$^{2-}$** with CO_2 in THF-d_8. Top: Portion of the ^{1}H,^{13}C HMBC NMR spectrum. Bottom: ^{13}C NMR spectrum including labelling scheme. Inset A: Strong enhancement of the resonance at 185 ppm in the reaction with $^{13}CO_2$ (black) compared to the reaction with non-enriched CO_2 (red). Spectra are normalized to the resonance at 20.3 ppm. Inset B: Splitting of the resonance at 75 ppm in the reaction with $^{13}CO_2$. *: pentane; #: $^{13}CO_2$ incorporation in side/decomposition products.

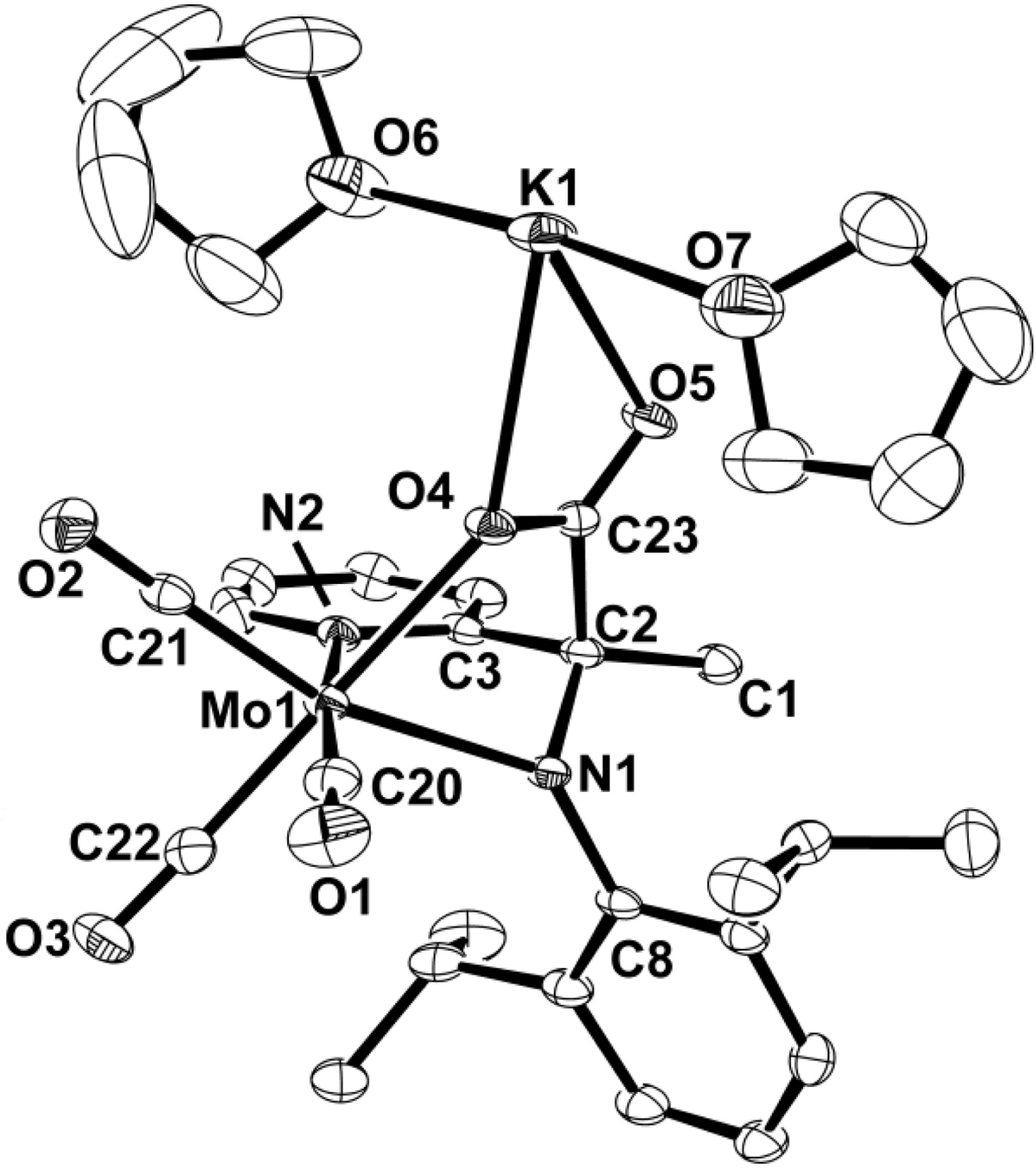

Figure 6.

Ortep diagram of the molecular structure of "**[$^{i\mathrm{Pr2Ph}}$PMI-Mo(CO)$_3$(CO$_2$)]K**" with ellipsoids shown at the 50% probability level. Hydrogen atoms and the co-crystallized, non-coordinated THF molecule are omitted for clarity. Selected bond length (Å) and angles (°): Mo(1)-N(1) 2.365(3), Mo(1)-N(2) 2.272(3), Mo(1)-C(20) 1.948(4), Mo(1)-C(21) 1.910(4), Mo(1)-C(22) 1.933(4), Mo(1)-O(4) 2.283(2), C(20)-O(1) 1.173(5), C(21)-O(2)1.181(4), C(22)-O(3) 1.178(5), C(23)-O(4) 1.273(4), C(23)-O(5) 1.230(4), O(4)-K(1) 2.834(2), O(5)-K(1) 2.748(3), N(1)-C(2) 1.527(5), C(2)-C(3) 1.523(5), C(2)-C(23) 1.572(5), N(1)-Mo(1)-

C(21) 164.17(13), N(2)-Mo(1)-C(20) 173.64(13), N(1)-Mo(1)-N(2) 73.76(10), N(2)-Mo(1)-C(21) 101.81(13), N(1)-Mo(1)-C(20) 100.23(14), C(20)-Mo(1)-C(21) 84.54(16), C(22)-Mo(1)-O(4) 175.56(13), N(1)-Mo(1)-C(22) 110.25(12), C(21)-Mo(1)-C(22) 85.17(15), O(4)-Mo(1)-C(21) 96.60(13), N(1)-Mo(1)-O(4) 67.77(9), Mo(1)-C(21)-O(2) 177.5(3), Mo(1)-C(20)-O(1) 176.0(4), Mo(1)-C(22)-O(3) 176.1(3), Mo(1)-O(4)-C(23) 116.9(2), O(4)-C(23)-O(5) 125.8(3), C(2)-C(23)-O(4) 114.8(3), C(2)-C(23)-O(5) 119.4(3), C(1)-C(2)-N(1) 114.4(3), C(1)-C(2)-C(3) 114.0(3), C(1)-C(2)-C(23) 111.3(3), N(1)-C(2)-C(3) 109.3(3), N(1)-C(2)-C(23) 104.1(3), C(3)-C(2)-C(23) 102.5(3), C(8)-N(1)-C(2) 115.3(3), Mo(1)-N(1)-C(8) 137.2(2), Mo(1)-N(1)-C(2) 101.51(19), O(4)-K(1)-O(5) 47.02(7).

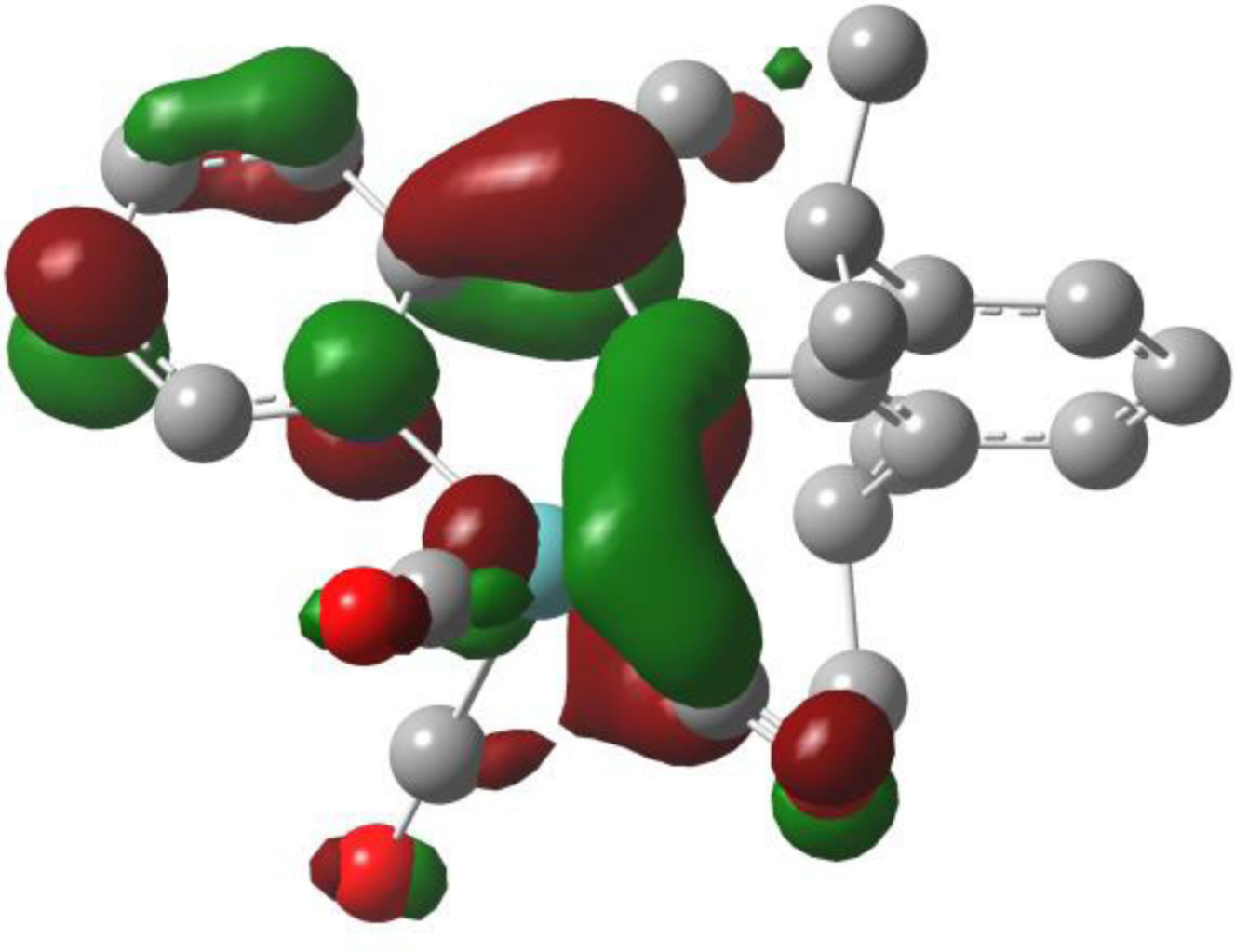

Figure 7.

The optimized geometry of **[^{iPr2Ph}PMI-Mo(CO)$_3$]$^{2-}$** with the overlaid HOMO (iso value = 0.04). Hydrogen atoms have been removed for clarity.

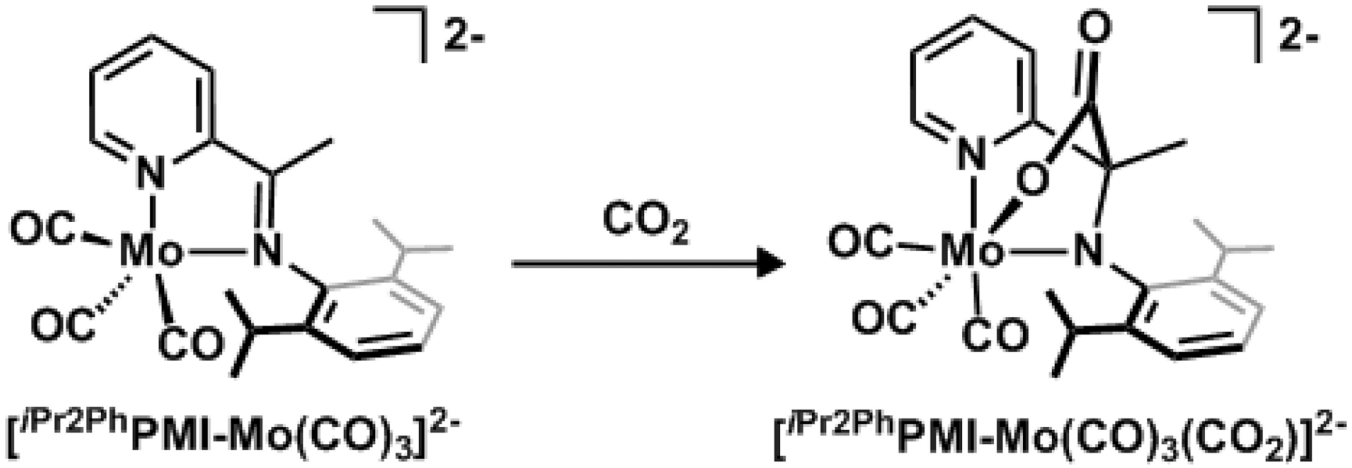

[^{i}Pr2Ph PMI-Mo(CO)$_3$]$^{2-}$ [^{i}Pr2Ph PMI-Mo(CO)$_3$(CO$_2$)]$^{2-}$

Scheme 1.

Proposed reaction path for the reaction of the dianion **[^{i}Pr2Ph PMI-Mo(CO)$_3$]$^{2-}$** with CO_2

Table 1

FTIR C≡O stretching vibrations[a] (cm^{-1}) and $E_{1/2}$ (V vs. Cp_2Fe in MeCN) of the complexes **bipy-Mo(CO)$_4$**, **^{Ph}PMI-Mo(CO)$_4$** and **^{iPr2Ph}PMI-Mo(CO)$_4$**.

Ligand:	Bipy[9]	^{Ph}PMI	^{iPr2Ph}PMI
ν(CO)	2016	2014	2011
	1904	1904	1899
	1877	1885	1883
	1832	1837	1839
$E_{1/2}$	−1.98	−1.80	−1.81
E_{cp}[b]	−2.54	−2.35	−2.55

[a] CH_3CN solutions.

[b] peak potential of the irrev. 2nd red. at 100 mV/s.